J Mater Sci: Mater Med (2011) 22:969–976
DOI 10.1007/s10856-011-4266-y

Biomechanical evaluation of regenerating long bone by nanoindentation

Takuya Ishimoto · Takayoshi Nakano · Masaya Yamamoto · Yasuhiko Tabata

Received: 21 August 2010 / Accepted: 17 February 2011 / Published online: 1 March 2011

Abstract It is crucial to measure the mechanical function of regenerating bone in order to assess the mechanical performance of the regenerating portion as well as the efficiency of the regeneration methods. In this study, nanoindentation was applied to regenerating and intact rabbit ulnae to determine the material properties of hardness and elasticity; viscoelasticity was also investigated to precisely evaluate the material properties. Both intact and regenerating bones exhibited remarkable viscoelasticity manifested as a creep behavior during load hold at the maximum load, and the creep was significantly greater in the regenerating bone than the intact bone. The creep resulted in an overestimation of the hardness and Young's modulus. Hence, during nanoindentation testing of bones, the effect of creep should be eliminated. Moreover, the regenerating bone had lower hardness and Young's modulus than the intact bone. The nanoindentation technique proved to be a powerful approach for understanding the mechanical properties of regenerating bone.

1 Introduction

In the field of orthopedics, it is vital to measure intrinsic mechanical properties of regenerating bone or fracture callus in order to investigate the mechanical integrity of the portion being healed and to validate the methods and medicines used for bone regeneration. Conventional mechanical tests such as tension, compression, bending, and torsion tests are commonly used to mechanically assess healing bones [1, 2]. In some cases, however, it is difficult to use these tests to assess material properties in detail, such as hardness and elasticity, because the mechanical outputs include the effects of macroscopic bone geometry. In addition, bone regeneration usually progresses non-uniformly with respect to size and shape, especially in the initial stage of bone healing; this makes it more difficult to use conventional mechanical tests to precisely measure the material properties of regenerating bone.

Recently, nanoindentation technique was developed and is currently widely used for evaluating the material properties of thin films, coating materials, and substances having a microstructure [3]. Nanoindentation testing produces a load–depth curve, and enables the determination of hardness and Young's modulus; viscoelastic behaviors (e.g., creep) can be analyzed from the load–depth curve. Nanoindentation does not necessarily require large and well-arranged specimens because the volume involved in the test is very small. Therefore, nanoindentation can be a powerful tool for characterizing the material properties of biological hard tissues. Many studies have evaluated the hardness and Young's modulus of biological hard tissues by using nanoindentation, mainly on intact bones with a focus on bone type (e.g., cortical and cancellous bones) [4, 5], microstructures (e.g., osteons and interstitial lamellae) [6–8], degree of mineralization [9], anisotropy [5, 10, 11], and specimen conditions of humidity and embedment [7, 12–14]. Thus, a wide range of the material properties of bone tissues has been revealed. To our knowledge, however, few nanoindentation studies have evaluated the material properties of bone in abnormal states, such as

T. Ishimoto · T. Nakano (✉)
Division of Materials and Manufacturing Science, Graduate School of Engineering, Osaka University, 2-1, Yamada-oka, Suita, Osaka 565-0871, Japan
e-mail: nakano@mat.eng.osaka-u.ac.jp

M. Yamamoto · Y. Tabata
Institute for Frontier Medical Sciences, Kyoto University, 53, Kawahara-cho, Shogoin, Sakyo-ku, Kyoto 606-8507, Japan

the pathologic [15, 16] and regenerative [17–20] states. Detailed information on these states is scarce. It is crucial to understand the intrinsic mechanical properties of these types of bones in clinical situations in order to diagnose the biomechanical performance of the skeleton.

In most nanoindentation studies, hardness and Young's modulus are predominantly analyzed from the unloading curve by using the method proposed by Oliver and Pharr [21], which is based on elastic contact mechanics. When this method is used for bone having time-dependent mechanical behavior [22], however, the viscoelasticity induces a remarkable impediment that results in inaccurate values of hardness and Young's modulus. For example, a negative stiffness was reported to appear because of a creep effect during initial unloading [23]. To overcome this problem, several techniques to exhaust the viscoelastic behavior of bone are used in the nanoindentation procedure. The multiple loading-and-unloading scheme [5–7], introduction of a constant load hold at the maximum load before unloading [5, 9, 11, 15, 16, 18–20, 24], rapid unloading [24, 25], and a combination of them [5, 24] can reduce the effect of bone viscoelasticity (creep) on the unloading curve and the resultant values of hardness and Young's modulus. As an alternative method, Oyen et al. [23] developed an analytical approach in which the nanoindentation load–depth curve is fitted under the assumption that specimen deformation is linear viscoelastic and the total indentation depth can be divided into 3 independent elements: elastic, plastic, and viscous. With this model, the hardness and Young's modulus of some kinds of intact mammalian bone [26] as well as healing bone near dental implants in miniswine alveolar bone [17] could be successfully determined, independent of the viscoelastic parameters of the bone. Ngan et al. [25, 27] also proposed a numerical method to correct for the creep effect. They modified the contact stiffness defined by an initial slope of unloading curve, based on the loading rate and displacement rate just before the unloading, and unloading rate, all of which can be obtained from load–depth data. By applying this model to mouse limb bones, the hardness and Young's modulus could be accurately calculated despite the appearance of the viscoelastic effect during unloading [25].

The ultimate goal of the current study is to evaluate the hardness and Young's modulus of regenerating bone tissue at 2 weeks of regeneration (very early stage of bone regeneration) as well as intact bone as a control by using nanoindentation. As mentioned above, in order to obtain the correct values of hardness and Young's modulus, it is necessary to diminish creep behavior, which inevitably appears during nanoindentation unloading. We focused on the constant load hold at the maximum load before unloading to diminish creep behavior in this study, because many nanoindentation studies on biological tissues have utilized this simple method. Especially in the early stage of regeneration, regenerating bone tissue may be highly viscoelastic because of its low mineralization level [28] and high fraction of organic collagen [29], which is believed to be a major factor contributing to bone viscoelasticity [30]. However, the viscoelastic behavior of regenerating bone during nanoindentation testing and its effects on hardness and Young's modulus are not necessarily considered [19]. Hence, this study also aims to estimate the time-dependent creep behavior in regenerating bone and its effect on hardness and Young's modulus as well as to determine suitable nanoindentation conditions for bone in the early stage of regeneration.

2 Materials and methods

2.1 Specimen preparation

All animal care and experiments were performed in accordance with the Guidelines of Animal Experiment of Institute for Frontier Medical Sciences, Kyoto University. Sample were obtained from the ulnar middiaphysis of a mature male New Zealand white rabbit weighing about 3 kg. With the animal under anesthesia, a 20-mm-long complete defect was prepared on the left ulnar middiaphysis with a surgical oscillating saw according to an established procedure [31]; the opposite ulna was left intact. After 2 weeks, the rabbit was sacrificed by an intravenously administered overdose of sodium pentobarbital. Both ulnae were removed, and bone mineral density (BMD) was assessed by peripheral quantitative computed tomography (pQCT) (XCT Research SA+; Stratec Medizintechnik GmbH, Birkenfeld, Germany) on the cross-sections around the center of the defect of the regenerating (left) and the corresponding sites (right). Bone tissue was judged over a threshold BMD value of 267 mg/cm^3 [32]. The bone specimens were sectioned into 2-mm slices perpendicular to the long bone axis by using a circular saw (Model 660; South Bay Technology Inc., San Clemente, CA, USA) with a diamond wheel to expose surfaces for the nanoindentation testing. The specimen surfaces were polished with abrasive papers of progressively finer grids (600, 800, and 1200) and finished with a 0.05-μm alumina suspension under deionized water. Finally, the samples were ultrasonically cleaned in deionized water for 5 min to remove debris on the surface. The water temperature was kept below 37°C during the ultrasonic exposure to prevent alterations in the mechanical properties of the bone.

The bone sections were dried in air for 1 day at room temperature. Mineralization of the regenerating tissues was analyzed by micro-focused X-ray computed tomography (μCT) (SMX-100CT; Shimadzu Co., Kyoto, Japan).

Nanoindentation measurement was conducted only on the mineralized part, which was identified on the basis of the μCT image. Cartilage and other soft tissues were not examined in this study. The specimens were fixed on a specimen holder and kept in a temperature-controlled chamber at the experimental temperature of 25°C for 24 h for thermal stabilization before nanoindentation testing.

2.2 Nanoindentation

The nanoindentation measurements were performed using a load-control-type nanoindentation system (ENT-1100a; Elionix Ltd., Tokyo, Japan). A diamond Berkovich pyramidal indenter was used for all measurements. The hardness and Young's modulus were calculated from the load–depth data using the method documented by Oliver and Pharr [21]. The hardness (H) and reduced modulus (E_r) were calculated from the following equations:

$$H = \frac{P_{max}}{A_c}$$

and

$$E_r = \frac{\sqrt{\pi}}{2\beta\sqrt{A_c}}S,$$

where P_{max} is the maximum load applied during testing, β is the empirical constant depending on the indenter geometry (equal to 1.034 for Berkovich indenter), S is the contact stiffness defined by the initial slope of the unloading curve (dP/dh), and A_c is the projected contact area as a function of contact depth (h_c). In this nanoindentation system, the calculation of A_c was modified by correcting the frame compliance and tip penetration depth using the method proposed by Sawa and Tanaka [33]. The contact depth, h_c, is defined by

$$h_c = h_{max} - \varepsilon\frac{P_{max}}{S}$$

where h_{max} is the maximum penetration depth and ε is a constant equal to 0.75 for Berkovich indenter. Finally, E_r is determined by a combination of the specimen modulus (E_s) and the indenter modulus (E_i) as follows:

$$\frac{1}{E_r} = \frac{1-\nu_s^2}{E_s} + \frac{1-\nu_i^2}{E_i}$$

where ν_s and ν_i are the Poisson ratio of the specimen and indenter, respectively. For the diamond indenter, E_i is 1140 GPa and ν_i is 0.07; ν_s for the bone specimen was assumed to be 0.3 [4].

Nanoindentation measurements were performed under a trapezoidal loading condition. The constant loading/unloading rate and maximum load (P_{max}) were 400 μN/s and 6 mN, respectively [34]; accordingly, the time for loading/unloading was 15 s. One of the objectives of this study was to precisely evaluate the hardness and Young's modulus of the regenerating bone and intact bone by minimizing the effect of the viscoelastic deformation of the bone, which appears during unloading. To minimize such viscoelastic behavior of the bone as creep, load hold at the maximum load for an adequate period is commonly used before unloading. The load hold period at the maximum load was set from 0 to 240 s to assess the effect of creep on hardness and elasticity. In addition, the load hold at the maximum load was used to observe the creep behavior itself. The upper part of the unloading curve from 50 to 95% of the maximum load was used for determining S [34] by fitting with a power function [21]. For each load hold condition, indentation was carried out 5 times along the long bone axis, and the mechanical parameters were averaged. All indentation points were located on the mineralized region of the intact ulna (Fig. 1a) and regenerating bone (Fig. 1b) near the radius, as determined from the μCT image. Osteocyte lacunae were avoided by observation using a CCD microscope attached to the nanoindentation system.

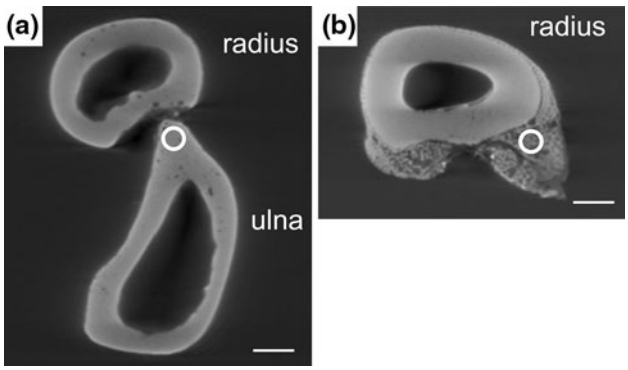

Fig. 1 μCT cross-sectional images of **a** the intact and **b** regenerating bone for which nanoindentation analysis was performed. Only the mineralized regions are shown. Indents were placed on the ulna near the neighboring radius in the intact site and the newly formed bone in the regenerating site, as indicated by *white circles*. The *scale bar* corresponds to 1 mm

2.3 Statistical analysis

All data were presented as means ± standard deviation (SD). Statistical comparison between the 2 means was performed using a two-tailed t test. The values of additional penetration depth, hardness, and Young's modulus for the intact and regenerating bones were compared using one-way analysis of variance (ANOVA). The level of significance was set at $P < 0.05$. The Statistical Package for Social Study (SPSS) version 14.0J software (SPSS Japan Inc., Tokyo, Japan) for Microsoft Windows was used for all statistical analyses.

3 Results

Figure 1 shows the μCT images of the intact and regenerating bone taken at the cross-section at which the nanoindentation measurements were performed. In the defect, there were very small amounts of mineralized bone tissue only along the radius at 2 weeks postoperatively. The BMD of the regenerating bone (430 mg/cm^3) was much lower than that of the intact bone (1,040 mg/cm^3). Conventional mechanical tests could not be conducted for the newly formed portion. The circles in Fig. 1 indicate the location at which the nanoindentation measurements were performed.

Figure 2 shows the typical nanoindentation load–depth curves obtained along the longitudinal axis for the intact bone with and without a load hold at the maximum load. Without the load hold, an overhanging portion, indicated by the arrow in Fig. 2, appeared at the beginning of the unloading curve because of the creep behavior under the load. The overhanging portion in the figure disappeared after the load hold at the maximum load was applied for a sufficient period before unloading. Load–depth curves obtained when load hold at the maximum load was applied for both the intact and regenerating bones are shown in Fig. 3. A clear difference can be seen in the indentation depth. The regenerating bone had a greater indentation depth than the control bone under the same maximum load. The regenerating bone showed less ability to resist deformation.

Figure 4 shows the change in the additional penetration depth caused by creep behavior as a function of the period of load hold at the maximum load. The additional penetration depth corresponds to the length of the arrowed segment in the inset of Fig. 4. The creep rate is represented by the slope of the tangent line in the additional penetration depth during the period of load hold at the maximum load. The initial creep rate was high when a constant load was applied; therefore, the additional penetration depth was high at the start of the load hold period. However, the creep rate decreased with the load hold period, and the total penetration became constant after a load hold period of 180 s for both the intact and regenerating bones. No significant changes were found in the additional penetration depth at a period of load hold at the maximum load exceeding 180 s. The regenerating bone exhibited significantly larger creep than the intact bone ($P < 0.001$ by one-way ANOVA).

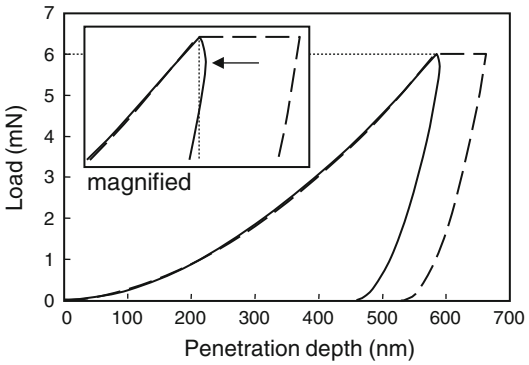

Fig. 2 Load–depth data for intact bone without (*solid line*) and with (*dashed line*) load hold at the maximum load for an adequate period. The measurements were performed along the longitudinal direction of the rabbit ulnae. In the absence of load hold at the maximum load, an overhanging portion, indicated by the *arrow*, appears on the upper part of the unloading curve because of creep; the insertion of load hold for an adequate period before unloading diminishes the creep effect on the unloading curve

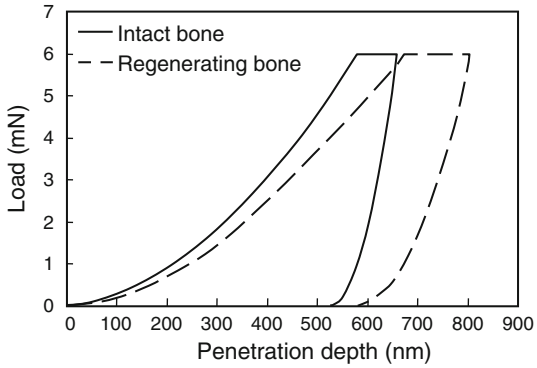

Fig. 3 Typical load–depth data for the intact (*solid line*) and regenerating bone (*dashed line*) measured along the longitudinal direction of rabbit ulnae. The regenerating bone exhibits greater penetration depth than the intact bone

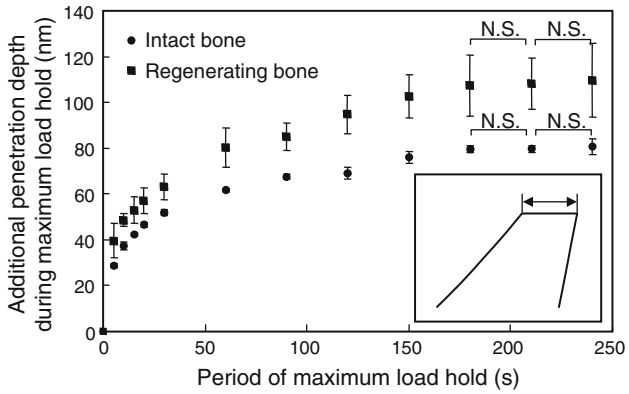

Fig. 4 Change in additional penetration (indicated by an *arrow in inset*, *bottom right*) during load hold at the maximum load for the intact (*filled circles*) and regenerating (*filled squares*) bone tissues. Additional penetration results from creep of bone tissue. The regenerating bone shows significantly greater additional penetration than the intact bone ($P < 0.001$ by one-way ANOVA). The creep rate diminishes gradually as a function of the load hold period, and the creep becomes constant after a load hold period of 180 s. N.S. indicates not significant

Figures 5 and 6 show the changes in the calculated values of hardness and Young's modulus as a function of the period of load hold at the maximum load, respectively. For both the intact and regenerating bones, relatively high values of hardness (819 MPa for the intact bone and 580 MPa for the regenerating bone) and Young's modulus (29.8 GPa for the intact bone and 20.7 GPa for the regenerating bone) were obtained when the load hold at the maximum load was not performed. The hardness and Young's modulus reduced to constant values after a load hold period excessing 60 s. The constant values of hardness were 695 and 486 MPa and those of Young's modulus were 27.6 and 17.0 GPa for the intact and regenerating bones, respectively. The hardness was overestimated because of the viscoelastic creep by 18 and 19% for the intact and regenerating bone, respectively; the corresponding values for Young's modulus were 8 and 22%. The regenerating bone showed significantly lower constant hardness and Young's modulus values than the intact bone ($P < 0.001$ by one-way ANOVA).

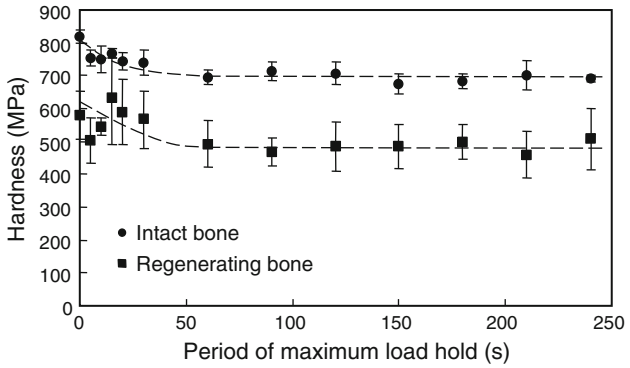

Fig. 5 Change in hardness as a function of the period of load hold at the maximum load for the intact (*filled circles*) and regenerating (*filled squares*) bone tissues. This graph represents the effect of creep on hardness, which appears on the unloading part of the load–depth curve. The hardness becomes constant after a load hold period exceeding 60 s. This graph also shows that the regenerating bone had a significantly lower hardness than intact bone ($P < 0.001$ by one-way ANOVA)

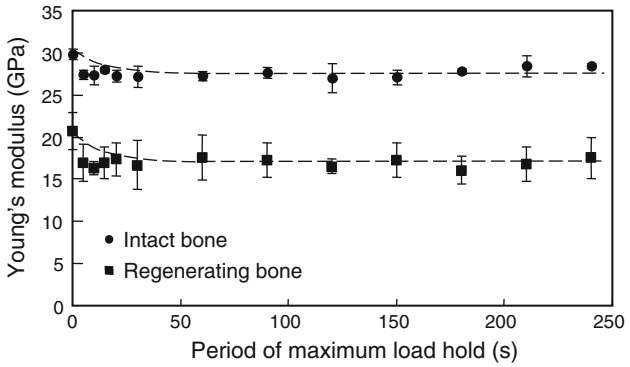

Fig. 6 Change in Young's modulus as a function of the period of load hold at the maximum load for the intact (*filled circles*) and regenerating (*filled squares*) bone tissues. This graph represents the effect of creep on Young's modulus, which appears on the unloading part of the load–depth curve. The Young's modulus becomes constant after a load hold period of 60 s and more. This graph also shows that the regenerating bone has a significantly lower Young's modulus than intact bone ($P < 0.001$ by one-way ANOVA)

4 Discussion

Nanoindentation is a useful technique for quantitatively measuring the material properties of regenerating bone as well as intact bone because the material properties can be analyzed even with small specimens. In this study, material properties were investigated using the nanoindentation procedure; loading, load hold at the maximum load, unloading, and important mechanical aspects of the regenerating bone tissue were revealed.

Bone tissue, which is mainly composed of an inorganic biological apatite crystal and an organic collagen fiber, is known to be viscoelastic [12, 22, 24, 35] largely because of the viscoelastic nature of organic collagen [30, 36]. Viscoelasticity is generally characterized by the creep and relaxation behaviors of materials, which are defined as an increase in strain with time under a constant stress and a decrease in stress with time under a constant strain, respectively. In nanoindentation testing, therefore, creep behavior can be observed during the period of load hold period at the maximum load as an increase in the additional penetration depth. In this study, clear creep behavior was observed in both the intact and regenerating bone tissues. The regenerating bone exhibited significantly greater creep than the intact bone (Fig. 3). This may be because the degree of mineralization was much lower in the regenerating bone as indicated by its lower BMD; hence, regenerating bone tissue is greatly affected by the viscoelasticity of the collagen matrix.

With the regenerating bone, which exhibited greater viscoelasticity, the overestimation of the hardness and Young's modulus tended to be greater without the load hold at the maximum load compared to the intact bone (Figs. 5, 6). In general, the viscoelastic behavior of specimen materials should be eliminated in order to appropriately evaluate the hardness and Young's modulus [37]. The effect of the viscoelastic behavior of bone tissue appears on the upper part of the unloading curve as an overhanging line, a so-called "nose." Because of this effect, the contact stiffness S, is miscalculated, and the hardness and Young's modulus determined are erroneous. In nanoindentation testing, the load hold at the maximum load before unloading plays the role of removing the effect of creep on the hardness and Young's modulus by enabling

the material to develop creep to a negligible rate. If the load hold period is insufficient, a nose appears on the upper part of the unloading curve (Fig. 2). The hardness and Young's modulus calculated from an overhanging unloading curve are not reliable [23]. The period of load hold at the maximum load before unloading must be adequate to bring the creep to a negligible rate. In this study, a load hold period of at least 60 s was required to avoid overestimating the hardness and Young's modulus in both the intact and regenerating bones. These findings strongly suggest that elimination of the effect of creep should be carefully considered during nanoindentation measurement of bone because bone material is highly viscoelastic. Furthermore, a long load hold period is necessary to correctly determine material properties.

For bone mechanics, viscoelastic behavior itself is also important; however, in this study, it was measured for the appropriate analysis of the hardness and Young's modulus. Bone's viscoelasticity strongly contributes to its toughness, which represents resistance to fracture [38]. Simulation models that enable direct analysis of the viscoelasticity-related parameters of bone were recently proposed. For example, the analytical model developed by Oyen et al. [17, 23, 26] enabled the determination of viscosity during trapezoidal loading nanoindentation procedures, which revealed the role of bone viscosity in plastic deformation resistance [26]. Ferguson [39] applied this model to horse metacarpal cortices, demonstrating the quantitative fraction of viscous deformation in the overall deformation. Rheological models consisting of springs and dashpots have also explored the viscous and/or viscoelastic response of biological mineralized tissues such as bone and tooth enamel [40, 41]. These techniques can be effectively used to understand how bone exhibits such time-dependent deformation behavior from the structural and compositional perspectives [42].

The effect of specimen drying on the absolute values of the material properties should be mentioned. Fully dried bone specimens were used in this study. Because of the removal of water, the hardness and Young's modulus are increased [7, 14] and creep deformation is reduced [42, 43] in dry specimens compared to wet specimens. When bone is dried, collagen shrinks and the bone tissue subsequently contracts [44, 45]. As a result, the apparent packing density of the bone tissue increases. This may be a possible reason why the material properties of bone change after drying. However, the relationship between the relative magnitudes of the material properties must be consistent even after specimens are dried, as confirmed by Rho and Pharr [7]. Another limitation of this study is the drift effect of hardware on mechanical properties. The drift effect is decoupled with the creep behavior resulting from viscoelasticity, which can ultimately result in increased ambiguity in the absolute value of material properties; to counteract this, the bone specimens and instrument were kept in a chamber at 25°C for 24 h before the testing for thermal stabilization. Although some instruments are specifically built to remove drift [46], a conventional nanoindentation instrument, which does not have this provision, was used in this study. Further study is needed to obtain quantitative absolute values of hardness and Young's modulus for solving problems related to drying, the drift effect, and the number of regenerative animals used.

As has also been reported previously [17, 18], the hardness and Young's modulus of the regenerating bone were significantly lower than those of the intact bone (Figs. 5, 6). It is widely recognized that variations in the material properties of bone are induced by variations in the micro-organizational features of bone tissue. Some researchers have proven the relationship between microscale organization and hardness and/or Young's modulus by using nanoindentation. Rho and Pharr [7] revealed that the hardness and Young's modulus of bovine femur cortical bone vary among microstructural components, including interstitial lamellae and osteons. Interstitial lamellae have higher values of hardness and Young's modulus along the longitudinal direction than osteons because of the higher degree of mineralization [9]. Turner et al. [5] demonstrated the anisotropy in Young's modulus of human femur cortical bone; the value of Young's modulus along the longitudinal direction was higher than that along the transverse direction. In cortical bone of a long bone, the collagen fibrils and the crystallographic *c* axis of biological apatite were found to be preferentially aligned along the longitudinal direction [47–49]. This could be a reason for the anisotropic Young's modulus in long bones, because collagen and biological apatite are anisotropic materials with respect to their mechanical properties [50, 51]. Jämsä et al. [15] reported that the cortical bone in the long bones of osteopetrotic rats exhibited lower elastic moduli than those of normal rats; this may be because of the degradation of microstructures, such as collagen cross-linkage and mineral crystallinity [52]. The organization and microstructure of regenerating long bones are also different from those of intact bones. For example, compared to a mature intact long bone, regenerating bone is less mineralized, contains a relatively high fraction of organic collagen [29], has low mineral crystallinity [53], and has randomly orientated collagen fibers [54] and mineral crystals [55, 56], especially in the early stage of regeneration. These microstructural features will definitely result in low hardness and Young's modulus values for regenerating bone tissue. Further investigation using nanoindentation to clarify the quantitative correlation between the bone microstructures mentioned above and material properties of regenerating bone is in progress.

5 Conclusions

Some mechanical behaviors of intact and regenerating bone tissue were characterized using the nanoindentation technique, and following conclusions were reached:

(1) In both intact and regenerating bones, remarkable viscoelasticity is observed as creep during the period of load hold at the maximum load. The creep is greater in the regenerating bone than in the intact bone, which may be because the former has a higher fraction of viscoelastic collagen matrix as a result of less mineralization. It takes 180 s to saturate the creep in both the intact and regenerating bones.

(2) The effects of creep appear as overestimation of the hardness and Young's modulus when load hold at the maximum load is not performed. The procedure of load hold at the maximum load effectively diminishes the effects of creep, which become negligible in both the intact and regenerating bones when the load hold period exceeds 60 s.

(3) The hardness and Young's modulus of the regenerating bone are significantly lower than those of the intact bone. This seems to be because of the difference in the organization and microstructure between regenerating and intact bones. However, the effects of microstructure on material properties should be clarified by further investigation.

Acknowledgments This work was supported by funds from the "Priority Assistance of the Formation of Worldwide Renowned Centers of Research—The Global COE Program (Project: Center of Excellence for Advanced Structural and Functional Materials Design)" and Grants-in-Aid for Scientific Research from the Japan Society for the Promotion of Science (JSPS) and the Ministry of Education, Culture, Sports, Science and Technology (MEXT) of Japan.

References

1. Watanabe Y, Takai S, Arai Y, Yoshino N, Hirasawa Y. Prediction of mechanical properties of healing fractures using acoustic emission. J Orthop Res. 2001;19:548–53.
2. Komatsubara S, Mori S, Mashiba T, Nonaka K, Seki A, Akiyama T, Miyamoto K, Cao Y, Manabe T, Norimatsu H. Human parathyroid hormone (1–34) accelerates the fracture healing process of woven to lamellar bone replacement and new cortical shell formation in rat femora. Bone. 2005;36:678–87.
3. Fischer-Cripps AC. Nanoindentation (mechanical engineering series). 2nd ed. Berlin: Springer; 2004.
4. Zysset PK, Guo XE, Hoffler CE, Moore KE, Goldstein SA. Elastic modulus and hardness of cortical and trabecular bone lamellae measured by nanoindentation in the human femur. J Biomech. 1999;32:1005–12.
5. Turner CH, Rho JY, Takano Y, Tsui TY, Pharr GM. The elastic properties of trabecular and cortical bone tissues are similar: results from two microscopic measurement techniques. J Biomech. 1999;32:437–41.
6. Rho JY, Zioupos P, Currey JD, Pharr GM. Variations in the individual thick lamellar properties within osteons by nanoindentation. Bone. 1999;25:295–300.
7. Rho JY, Pharr GM. Effects of drying on the mechanical properties of bovine femur measured by nanoindentation. J Mater Sci Mater Med. 1999;10:485–8.
8. Hoffler CE, Moore KE, Kozloff K, Zysset PK, Brown MB, Goldstein SA. Heterogeneity of bone lamellar-level elastic moduli. Bone. 2000;26:603–9.
9. Rho JY, Zioupos P, Currey JD, Pharr GM. Microstructural elasticity and regional heterogeneity in human femoral bone of various ages examined by nano-indentation. J Biomech. 2002;35:189–98.
10. Swadener JG, Rho JY, Pharr GM. Effects of anisotropy on elastic moduli measured by nanoindentation in human tibial cortical bone. J Biomed Mater Res. 2001;57:108–12.
11. Fan Z, Swadener JG, Rho JY, Roy ME, Pharr GM. Anisotropic properties of human tibial cortical bone as measured by nanoindentation. J Orthop Res. 2002;20:806–10.
12. Bembey AK, Oyen ML, Bushby AJ, Boyde A. Viscoelastic properties of bone as a function of hydration state determined by nanoindentation. Philos Mag. 2006;86:5691–703.
13. Guidoni G, Swain M, Jäger I. Nanoindentation of wet and dry compact bone: influence of environment and indenter tip geometry on the indentation modulus. Philos Mag. 2010;90:553–65.
14. Bushby AJ, Ferguson VL, Boyde A. Nanoindentation of bone: comparison of specimens tested in liquid and embedded in polymethylmethacrylate. J Mater Res. 2004;19:249–59.
15. Jämsä T, Rho JY, Fan Z, MacKay CA, Marks SC Jr, Tukkanen J. Mechanical properties in long bones of rat osteopetrotic mutations. J Biomech. 2002;35:161–5.
16. Silva MJ, Brodt MD, Fan Z, Rho JY. Nanoindentation and whole-bone bending estimates of material properties in bones from the senescence accelerated mouse SAMP6. J Biomech. 2004;37:1639–46.
17. Oyen ML, Ko C-C. Examination of local variations in viscous, elastic, and plastic indentation responses in healing bone. J Mater Sci Mater Med. 2007;18:623–8.
18. Pelled G, Tai K, Sheyn D, Zilberman Y, Kumbar S, Nair LS, Laurencin CT, Gazit D, Ortiz C. Structural and nanoindentation studies of stem cell-based tissue-engineered bone. J Biomech. 2007;40:399–411.
19. Leong PL, Morgan EF. Measurement of fracture callus material properties via nanoindentation. Acta Biomater. 2008;4:1569–75.
20. Tai K, Pelled G, Sheyn D, Bershteyn A, Han L, Kallai I, Zilberman Y, Ortiz C, Gazit D. Nanobiomechanics of repair bone regenerated by genetically modified mesenchymal stem cells. Tissue Eng A. 2008;14:1709–20.
21. Oliver WC, Pharr GM. An improved technique for determining hardness and elastic modulus using load and displacement sensing indentation experiments. J Mater Res. 1992;7:1564–83.
22. Garner E, Lakes R, Lee T, Swan C, Brand R. Viscoelastic dissipation in compact bone: implications for stress-induced fluid flow in bone. J Biomech Eng. 2000;122:166–72.
23. Oyen ML, Cook RF. Load–displacement behavior during sharp indentation of viscous–elastic–plastic materials. J Mater Res. 2003;18:139–50.
24. Fan Z, Rho JY. Effects of viscoelasticity and time-dependent plasticity on nanoindentation measurements of human cortical bone. J Biomed Mater Res A. 2003;67:208–14.
25. Tang B, Ngan AHW, Lu WW. Viscoelastic effects during depth-sensing indentation of cortical bone tissues. Philos Mag. 2006;86:5653–66.

26. Olesiak SE, Oyen ML, Ferguson VL. Viscous–elastic–plastic behavior of bone using Berkovich nanoindentation. Mech Time Depend Mater. 2010;14:111–24.
27. Ngan AHW, Wang HT, Tang B, Sze KY. Correcting power-law viscoelastic effects in elastic modulus measurement using depth-sensing indentation. Int J Solid Struct. 2005;42:1831–46.
28. Abbaspour A, Takata S, Sairyo K, Katoh S, Yukata K, Yasui N. Continuous local infusion of fibroblast growth factor-2 enhances consolidation of the bone segment lengthened by distraction osteogenesis in rabbit experiment. Bone. 2008;42:98–106.
29. Chakkalakal DA, Lippielloa L, Wilsona RF, Shindella R, Connollya JF. Mineral and matrix contributions to rigidity in fracture healing. J Biomech. 1990;23:425–34.
30. Sasaki N, Yoshikawa M. Stress relaxation in native and EDTA-treated bone as a function of mineral content. J Biomech. 1993; 26:77–83.
31. Yamamoto M, Takahashi Y, Tabata Y. Enhanced bone regeneration at a segmental bone defect by controlled release of bone morphogenetic protein-2 from a biodegradable hydrogel. Tissue Eng. 2006;12:1305–11.
32. Tanaka M, Sakai A, Uchida S, Tanaka S, Nagashima M, Katayama T, Yamaguchi K, Nakamura T. Prostaglandin E2 receptor (EP4) selective agonist (ONO-4819.CD) accelerates bone repair of femoral cortex after drill-hole injury associated with local upregulation of bone turnover in mature rats. Bone. 2004;34:940–8.
33. Sawa T, Tanaka K. Simplified method for analyzing nanoindentation data and evaluating performance of nanoindentation instruments. J Mater Res. 2001;16:3084–96.
34. Akhter MP, Fan Z, Rho JY. Bone intrinsic material properties in three inbred mouse strains. Calcif Tissue Int. 2004;75:416–20.
35. Isaksson H, Nagao S, Małkiewicz M, Julkunen P, Nowak R, Jurvelin JS. Precision of nanoindentation protocols for measurement of viscoelasticity in cortical and trabecular bone. J Biomech. 2010;43:2410–7.
36. Chaudhry B, Ashton H, Muhamed A, Yost M, Bull S, Frankel D. Nanoscale viscoelastic properties of an aligned collagen scaffold. J Mater Sci Mater Med. 2009;20:257–63.
37. Briscoe BJ, Fioli L, Pelillo E. Nano-indentation of polymeric surfaces. J Phys D Appl Phys. 1998;31:2395–405.
38. Anup S, Sivakumar SM, Suraishkumar GK. Influence of viscoelasticity of protein on the toughness of bone. J Mech Behav Biomed Mater. 2010;3:260–7.
39. Ferguson VL. Deformation partitioning provides insight into elastic, plastic, and viscous contribution to bone material behavior. J Mech Behav Biomed Mater. 2009;2:364–74.
40. Mencik J, He LH, Swain MV. Determination of viscoelastic–plastic material parameters of biomaterials by instrumented indentation. J Mech Behav Biomed Mater. 2009;2:318–25.
41. Zhang J, Niebur GL, Ovaert TC. Mechanical property determination of bone though nano- and micro-indentation testing and finite element simulation. J Biomech. 2008;41:267–75.
42. He LH, Swain MV. Understanding the mechanical behaviour of human enamel from its structural and compositional characteristics. J Mech Behav Biomed Mater. 2008;1:18–29.
43. He LH, Swain MV. Influence of environment on the mechanical behaviour of mature human enamel. Biomaterials. 2007;28: 4512–20.
44. Lees S, Bonar LC, Mook HA. A study of dense mineralized tissue by neutron diffraction. Int J Biol Macromol. 1984;6:321–6.
45. Finlay JB, Hardie WR. Anisotropic contraction of cortical bone caused by dehydration of samples of the bovine femur in vitro. J Eng Med. 1994;208:27–32.
46. Nohava J, Randall NX, Conté N. Novel ultra nanoindentation method with extremely low thermal drift: principle and experimental results. J Mater Res. 2009;24:873–82.
47. Nakano T, Kaibara K, Tabata Y, Nagata N, Enomoto S, Marukawa E, Umakoshi Y. Unique alignment and texture of biological apatite crystallites in typical calcified tissues analyzed by microbeam X-ray diffractometer system. Bone. 2002;31: 479–87.
48. Sasaki N, Sudoh Y. X-ray pole figure analysis of apatite crystals and collagen molecules in bone. Calcif Tissue Int. 1997;60: 361–7.
49. Nakano T, Tabata Y, Umakoshi Y. Texture and bone reinforcement (MS2061). In: Encyclopedia of materials, science and technology updates. Oxford: Elsevier; 2005. pp. 1–8.
50. Nakano T, Awazu T, Umakoshi Y. Plastic deformation and operative slop system in mineral fluorapatite single crystal. Scr Mater. 2001;44:811–5.
51. Viswanath B, Raghavan R, Ramamurty U, Ravishankar N. Mechanical properties and anisotropy in hydroxyapatite single crystals. Scr Mater. 2007;57:361–4.
52. Wojtowicz A, Dziedzic-Goclawska A, Kaminski A, Stachowicz W, Wojtowicz K, Marks SC Jr, Yamauchi M. Alteration of mineral crystallinity and collagen cross-linking of bones in osteopetrotic toothless (tl/tl) rats and their improvement after treatment with colony stimulating factor-1. Bone. 1997;20:127–32.
53. Yang X, Ricciardi BF, Hernandez-Soria A, Shi Y, Camacho NP, Bostrom MPG. Callus mineralization and maturation are delayed during fracture healing in interleukin-6 knockout mice. Bone. 2007;41:928–36.
54. Wen HB, Cui FZ, Geng QL, Li HD, Zhu XD. Microstructural investigation of the early external callus after diaphyseal fractures of human long bone. J Struct Biol. 1995;114:115–22.
55. Nakano T, Kaibara K, Tabata Y, Nagata N, Enomoto S, Marukawa E, Umakoshi Y. Analysis of hydroxyapatite (HAp) texture in regenerated hard tissues using micro-beam X-ray diffractometer technique. In: Ikada Y, Umakoshi Y, Hotta T, editors. Tissue engineering for therapeutic use 6. Amsterdam: Elsevier; 2002. p. 95–104.
56. Ishimoto T, Nakano T, Umakoshi Y, Yamamoto M, Tabata Y. Role of stress distribution on healing process of preferential alignment of biological apatite in long bones. Mater Sci Forum. 2006;512:261–4.